The 2009 IEEE/RSJ International Conference on
Intelligent Robots and Systems
October 11-15, 2009 St. Louis, USA

The Surface Walker : a Hemispherical Mobile Robot with Rolling Contact Constraints

Masato ISHIKAWA, Yoshinori KOBAYASHI, Ryohei KITAYOSHI and Toshiharu SUGIE

Abstract— **In this paper, we propose a new example of non-holonomic mobile robot, which we call *the surface walker*. This robot is composed of a hemisphere-shaped shell and a 2-d.o.f. mass-control device (pendulum) inside it, and undergoes the rolling contact constraint between the hemispherical surface of the robot and the ground. Unlike a lot of non-holonomic robots which have ever been researched, the drift term exists in the system of the hemisphere robot. First, we show basic concepts which the hemisphere robot has, and construct the kinetic model of this robot. Then we realize the locomotion control of the robot by periodically oscillating the internal pendulum and show its effectiveness by control experiments.**

I. INTRODUCTION

In the last decade, there have been several studies on sphere-shaped mobile robot([1]-[5]). Unlike the robots with feet or wheels as driving device, spherical mobile robots can move in all directions without turning around. By taking advantage of the shape, the robots can also move on a muddy swamp and we can provide more space where robots can travel with this sphere-shaped mechanism. While this sphere robot is useful for locomotion, it is impossible for the sphere-shaped robot with manipulators to roll on the ground because the shape specializes in movement. If this robot pulls out the manipulators for operation from the body, the robot can not move by using all of the surface and we must consider how this robot move with available part of the surface. In this case, this robot correspond to a hemisphere-shaped robot. It is necessary to consider how this robot moves. In addition, if we consider robots with manipulators, reaction moment which is generated by movement of manipulator is a burden to legs for the mobile manipulators which have feet or wheels. But the hemisphere robot with manipulators which we propose in this paper can take advantage of the reaction moment which is generated by movement of manipulator as coordinated motion by regarding the moment as the input for mobile robot.

In this study, we propose a hemispherical mobile robot, which we call the Surface Walker. The robot travels in constant direction by changing its own position in compliance with new transference principle obtained from the equation of constraint between the hemisphere and the floor. Surface Walker consists principally of hemispherical enclosure as a base and a pendulum consisting of combining two RC servo-motors. The pendulum generates 2-d.o.f. torque for its movement by activating this two RC servo-motors. The Surface Walker can change its own posture by using this pendulum.

The authors are with Dept. of Systems Science, Graduate School of Informatics, Kyoto university, 611-0011 Kyoto, Japan masato@i.kyoto-u.ac.jp

Most of the past studies on non-holonomic systems as the systems which have no momentum, or the system whose action drift term does not affect essentially[6]. Whereas, the hemisphere mobile robot belongs to a system with a drift term which affect the movement of the robot. Because of this drift term, it is difficult to find how to apply inputs into the robot for turning the state of the system into any states we want. Therefore, researchers have ever taken out the drift term in order to design the input for the intended state transition. The drift term affect on the state even if there is no input. Then the system with this term has capability of locomotion even if there is no input, or more effective movement.

This paper is organized as follows. First, we explain concept and overview of the Surface Walker and derive the dynamical model of the robot considering nonholonomic rolling contact constraint, in Section II. In Section III, we reduce the problem to a kinematic one in order to obtain a periodic control input for forwarding locomotion. Then we apply it to the original dynamical model and examine its validity by numerical simulations. Finally, in Section IV, we explain the experimental setup and verify the effectiveness of this movement mechanism from the experiment in which we apply the input used in the simulation the experimental setup. Section V concludes the article.

II. MODELING

A. Overview

The robot which has a hemispherical body as movement mechanism can not continue to roll in constant direction like the robots with spherical body, and it is difficult to understand movement principle intuitively. We call the hemisphere mobile robot as the Surface Walker, and we design and develop the robot in order to study the movement of the robot with this hemispherical body.

Let us call the pendulum-like mass control device *the arm block* from now on. A weight is fixed at the end of the arm block. The weight at the end can swing inside the hemisphere freely by controlling these two actuators.

In this section, we derive the model of the Surface Walker shown as Fig.1 from the design drawing shown as the Fig.2.

In the model of the Fig.3, we determine the location of the mass of the Surface Walker except the pendulum by considering that the mass exists upper side of the hemisphere because the microcomputer and the sensors placed above the hemisphere. In what follows, we derive the Euler-Lagrange

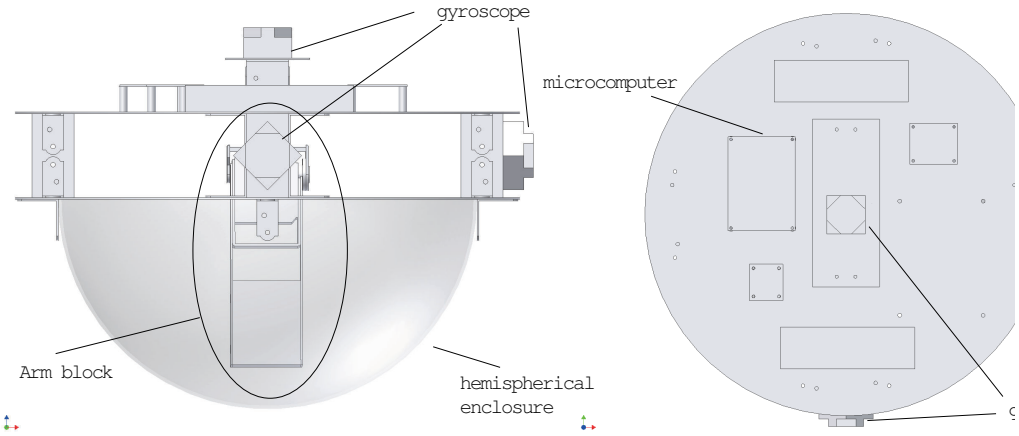

Fig. 1. The side and the top view of the Surface Walker

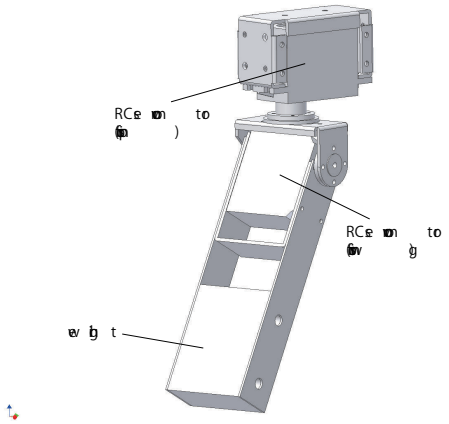

Fig. 2. Arm Block

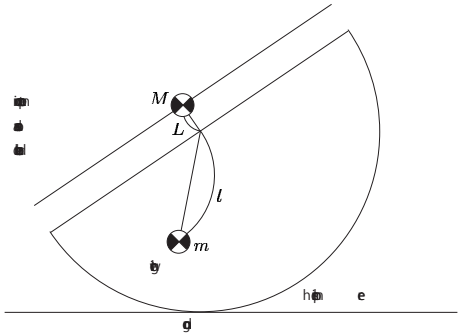

Fig. 3. Simplified Two-mass model of the Surface Walker

equation of motion and constraint between the hemisphere and the floor, and develop the model of the Surface Walker by combining them.

B. Orientation and Internal Shape

The robot has 3 degrees of freedom for its orientation as shown in Fig.4. To specify the coordinates, suppose N is the north pole of the globe, S is the south pole O is a point on the equator. The globe is cut into a hemisphere by a great circle passing through N and S, so that O is the bottom end. u_b, v_b are the latitude and longitude of the contact point P, respectively, and ψ is the angle formed by the x-axis on the floor and the the meridian passing through P. In other words, v_b is the roll, u_b is the pitch, and $-\psi$ is yaw of the Surface Walker.

The arm block has 2 degrees of freedom as shown in Fig.5, denoted by the position of the mass θ, ϕ with respect to the body coordinate.

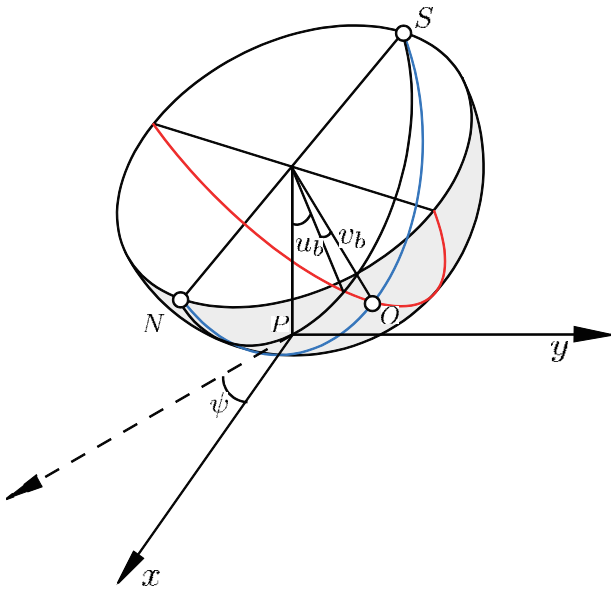

Fig. 4. Coordinate setting for orientation

C. Rolling Contact Condition

Let us consider the condition of rolling contact between the hemisphere and the floor. Throughout this paper, we assume that the sphere may roll over the floor and spin about the vertical axis, but never slips. Fig. 6 shows the sphere (instead of the hemisphere just to improve the visibility) put on the floor. O is the inertial frame where the floor coincides

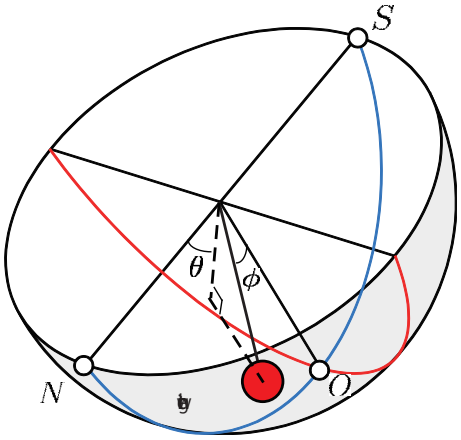

Fig. 5. Coordinate setting for the arm block

the x-y plane, C is a frame fixed to the sphere. For any point A on the sphere, let $r = \overrightarrow{CA}$, $q_0 = \overrightarrow{CO}$ and $q = \overrightarrow{OA}$, all expressed in the inertial coordinates.

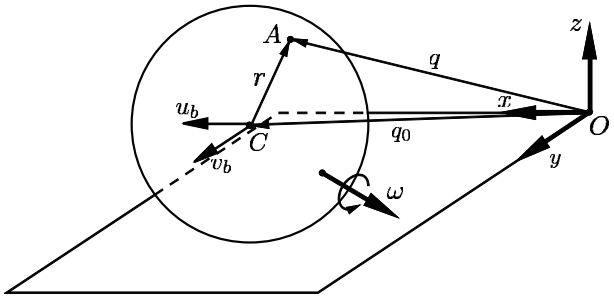

Fig. 6. Coordinate setting for rolling contact constraint

Then we have

$$q(t) = q_0(t) + r(t) \tag{1}$$

and its time derivative

$$\dot{q}(t) = \dot{q}_0(t) + \dot{r}(t) \tag{2}$$

Let $R(t)$ denote a 3×3 rotation matrix which describes the orientation of the sphere. Then the body coordinate r_C of the point A, is described as

$$r(t) = R(t) r_C \tag{3}$$

Then we take the following equation,

$$\frac{dR}{dt} = \begin{pmatrix} 0 & -\omega_3 & \omega_2 \\ \omega_3 & 0 & -\omega_1 \\ -\omega_2 & \omega_1 & 0 \end{pmatrix} R \tag{4}$$

and differentiate eq.(3) with respect to time.

$$\frac{dr(t)}{dt} = \frac{dR}{dt} r_C = \hat{\omega} R(t) r_C \tag{5}$$

$$= \hat{\omega} r(t) \tag{6}$$

Here $\hat{\omega}$ corresponds to the skew-symmetric matrix of ω.

Let us consider the two special cases. From Fig. 4, the velocity of the center C is

$$\dot{q} = \begin{pmatrix} \cos(-\psi) & -\sin(-\psi) & 0 \\ \sin(-\psi) & \cos(-\psi) & 0 \\ 0 & 0 & 1 \end{pmatrix} \begin{pmatrix} \rho \dot{u}_b \\ \rho \cos u_b \cdot \dot{v}_b \\ 0 \end{pmatrix} \tag{7}$$

at $r = (0,0,0)^T$, where ρ is the radius of the sphere. Second, since the contact point does not move instantaneously, we have

$$\dot{q} = (0,0,0)^T \quad \text{at} \quad r = (0,0,-\rho)^T \tag{8}$$

Substituting (7)(8) to (2)(6), we have

$$\begin{pmatrix} \rho \cos\psi \cdot \dot{u}_b - \rho \sin\psi \cos u_b \cdot \dot{v}_b \\ -\rho \sin\psi \cdot \dot{u}_b - \rho \cos\psi \cos u_b \cdot \dot{v}_b \\ 0 \end{pmatrix} = \begin{pmatrix} \dot{x} \\ \dot{y} \\ 0 \end{pmatrix} + \omega \times \begin{pmatrix} 0 \\ 0 \\ 0 \end{pmatrix}$$

$$\begin{pmatrix} 0 \\ 0 \\ 0 \end{pmatrix} = \begin{pmatrix} \dot{x} \\ \dot{y} \\ 0 \end{pmatrix} + \omega \times \begin{pmatrix} 0 \\ 0 \\ -\rho \end{pmatrix}$$

By eliminating ω_1, ω_2 from these equations, we obtain the following kinematic constraint

$$\begin{pmatrix} \dot{u}_b \\ \dot{v}_b \\ \dot{x} \\ \dot{y} \\ \dot{\psi} \end{pmatrix} = \begin{bmatrix} \frac{1}{\rho}\cos\psi & -\frac{1}{\rho}\sin\psi & 0 \\ -\frac{1}{\rho}\sec u_b \sin\psi & -\frac{1}{\rho}\sec u_b \cos\psi & 0 \\ 1 & 0 & 0 \\ 0 & 1 & 0 \\ \frac{1}{\rho}\tan u_b \sin\psi & \frac{1}{\rho}\tan u_b \cos\psi & -1 \end{bmatrix} \begin{pmatrix} \dot{x} \\ \dot{y} \\ \dot{w}_b \end{pmatrix} \tag{9}$$

where w_b is an augmented generalized coordinate, defined as a solution of the following differential equation

$$\dot{w}_b = \omega_3 \tag{10}$$

The constraint (9) can be rewritten in the matrix form

$$J(q_s)\dot{q}_s = 0 \tag{11}$$

where

$$J(q_s) = \begin{pmatrix} 1\,0\,0\,0\,0 & -\frac{1}{\rho}\cos\psi & \frac{1}{\rho}\sin\psi & 0 \\ 0\,1\,0\,0\,0 & \frac{1}{\rho}\sec u_b \sin\psi & \frac{1}{\rho}\sec u_b \cos\psi & 0 \\ 0\,0\,0\,0\,1 & -\frac{1}{\rho}\tan u_b \sin\psi & -\frac{1}{\rho}\tan u_b \cos\psi & 1 \end{pmatrix} \tag{12}$$

$$q_s = \begin{pmatrix} u_b & v_b & \theta & \phi & \psi & x & y & w_b \end{pmatrix}^T \tag{13}$$

Now we are ready to derive Euler-Lagrangian equation of motion by a standard manner (we omit the details of derivation). Using q_s as the generalized coordinates, we have

$$M(q_s)\ddot{q}_s + C(q_s, \dot{q}_s)\dot{q}_s + G(q_s) = B(q_s)\tau - J(q_s)^T \lambda \tag{14}$$

including the term for constraint force $-J(q_s)^T\lambda$, where λ is Lagrangian multiplier to determine.

The constrained Euler-Lagrange equation of motion can be solved by the following augmented differential equation

$$\left[\begin{array}{c|cc} I_{8\times8} & O_{8\times8} & O_{8\times3} \\ \hline O_{8\times8} & M(q_s) & J(q_s)^T \\ \hline O_{3\times8} & J(q_s) & O_{3\times3} \end{array}\right] \frac{d}{dt}\begin{pmatrix} q_s \\ \dot{q}_s \\ \gamma \end{pmatrix}$$

$$= \left[\begin{array}{c} I_{8\times8} \\ \hline -C(q_s,\dot{q}_s) \\ \hline -\dot{J}(q_s) \end{array}\right] \dot{q} + \left[\begin{array}{c} O_{8\times1} \\ \hline -G(q_s) \\ \hline O_{3\times1} \end{array}\right] + \left[\begin{array}{c} O_{8\times2} \\ \hline O_{2\times2} \\ I_{2\times2} \\ \hline O_{4\times2} \\ \hline O_{3\times2} \end{array}\right] \tau \quad (15)$$

The top 8 rows of this differential equation merely implies the correspondence

$$\frac{dq}{dt} = \dot{q},$$

and the following 8 rows is the Euler-Lagrange equation of motion (14) itself where λ is replaced by $\dot{\gamma}$. The bottom 3 rows imply the time derivative of the constraint condition, namely

$$J(q_s)\ddot{q}_s + \dot{J}(q_s)\dot{q}_s = 0 \quad (16)$$

III. Control Principle

A. Reduced Kinematic State Equation

In this subsection, we consider the forward locomotion of the Surface Walker. First, we derive the state equation based on the kinematics. Then we decide the forward locomotion input to the Surface Walker by using the state equation.

First, we consider the constraint between the pendulum and the posture of the hemisphere. The weight at the end of the pendulum is heavier than the other part of Surface Walker enough, and we suppose that the weight stays on the vertical axis at the contact point when the hemisphere moves. This assumption is reasonable for consideration of the Surface Walker's kinematics model because the momentum is small enough. We derive the following state equation under the assumption.

$$\begin{pmatrix} \dot{v}_b \\ \dot{u}_b \\ \dot{\psi} \\ \dot{x} \\ \dot{y} \\ \dot{\phi} \\ \dot{\theta} \end{pmatrix} = \begin{pmatrix} \cos v_b \tan u_b \\ -\frac{1}{\cos u_b}\sin\theta\sin\phi \\ -\cos v_b \sin u_b \tan u_b \\ -\cos v_b \sin u_b \sin\psi - \frac{1}{\cos u_b}\sin\theta\sin\phi\cos\psi \\ -\cos v_b \sin u_b \cos\psi + \frac{1}{\cos u_b}\sin\theta\sin\phi\sin\psi \\ 1 \\ 0 \end{pmatrix} \dot{\phi}$$

$$+ \begin{pmatrix} \frac{1}{\cos^2 u_b}\sin\phi \\ \frac{1}{\cos u_b}\cos\theta\cos\phi \\ -\frac{1}{\cos^2 u_b}\sin u_b \sin\phi \\ -\frac{1}{\cos u_b}\sin\phi\sin\psi + \frac{1}{\cos u_b}\cos\theta\cos\phi\cos\psi \\ -\frac{1}{\cos u_b}\sin\phi\cos\psi - \frac{1}{\cos u_b}\cos\theta\cos\phi\sin\psi \\ 0 \\ 1 \end{pmatrix} \dot{\theta} \quad (17)$$

We simplify this kinematics-based state equation as

$$\dot{\xi} = g_1\dot{\phi} + g_2\dot{\theta} \quad (18)$$

We consider the input for forward locomotion on the holonomy principle. Lie Bracket $[g_1, g_2]$ of g_1, g_2 in this state equation corresponds to the direction in which the Surface Walker moves on the floor. By using the holonomy principle, we can understand that the Surface Walker move straight with closed curve input on the $\dot{\phi}$-$\dot{\theta}$ plane.

B. Forward Locomotion

With the closed curve input on the $\dot{\phi}$-$\dot{\theta}$ plane derived in the previous section for the forward locomotion from a kinematic point of view, we realize the forward locomotion of the Surface Walker. Here, we apply periodic inputs

$$\phi_{\mathrm{ref}} = A_l \sin(\omega_l t + \pi/2) \quad (19)$$

$$\theta_{\mathrm{ref}} = B_l \sin\omega_l t \quad (20)$$

and simulate the forward locomotion with the state equation derived in Section II.

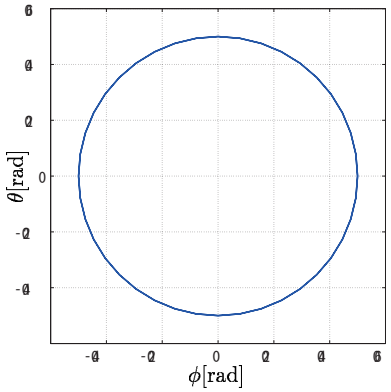

Fig. 7. Case 1:Periodic Reference to the Joints with small amplitude

These inputs are the reference angles of the RC servomotors of the pendulum. The movement of the Surface Walker with these inputs is kinematics-based, or the dynamics has little effect on the movement because the movement is slow enough . As a result of the simulation, the set of the contact point between the hemisphere and the floor on the x-y plane shows the following trajectory.

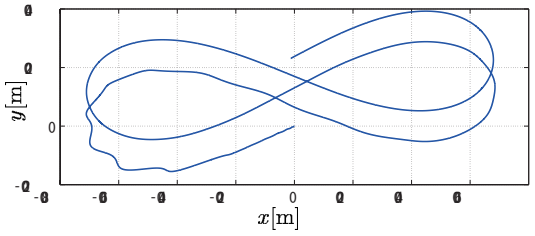

Fig. 8. Trajectory of the robot's position (x, y) in Case 1 (Kinematics is dominant - little dynamic effect)

Therefore, we verify that the input derived in the previous section is available. But there is an upper limit to the velocity

of the pendulum which can achieve kinematics-based motion of the Surface Walker.

Next, we consider another periodic input which keeps the mass closer to the center compared to the previous one. That is, we simulate the movement of the Surface Walker when the dynamic model has a big effect on the movement. For $t \in [0, \infty)$, we choose the following input:

If $0 \leq t \bmod 2\pi < \pi$

$$\begin{cases} \phi_{\text{ref}} & = A_s \sin 2\omega_s t \\ \theta_{\text{ref}} & = B_s/2 \sin(2\omega_s t - \pi/2) + B_s/2 \end{cases} \tag{21}$$

If $\pi \leq t \bmod 2\pi < 2\pi$

$$\begin{cases} \phi_{\text{ref}} & = A_s \sin 2\omega_s t \\ \theta_{\text{ref}} & = -B_s/2 \sin(2\omega_s t + \pi/2) - B_s/2 \end{cases} \tag{22}$$

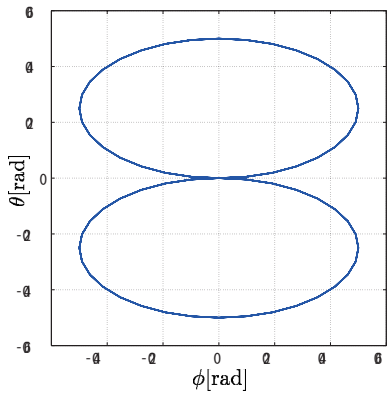

Fig. 9. Case 2:Periodic Reference to the Joints with large amplitude

In the Fig.9, the input pattern becomes closed curve on the $\dot{\phi}$, $\dot{\theta}$ plane, and this input satisfies a requirement for forward locomotion. The result of this simulation is shown as Fig.10.

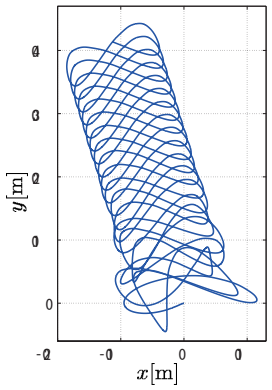

Fig. 10. Trajectory of the robot's position (x, y) in Case 2 (Kinematics is less dominant - large dynamic effect)

As a result of the simulation, the trajectory of the contact point is turbulent in the early stages and the Surface Walker moves straight from a certain moment, when the kinetics model has a big effect on the movement. We call this turbulent trajectory the scattering movement, and the stable trajectory which converge in a pattern the convergence movement. This scattering movement is affected by the drift term in the kinetic model which does not exist in the kinematics model.

IV. Experiment

A. Experimental Setup

Fig.11 illustrates an overview of our experiment system, and a portrait of the surface walker is shown in Fig.12. The body of the surface walker is a hemispherical transparent acrylic shell. The microcomputer, sensor processing circuit and other electronic devices are assembled on a black aluminum board above the shell. The arm block is a 2-d.o.f. manipulator actuated by two R/C servo motors, one for spin about the vertical axis and the other for swing motion. Both axes intersect at the center of the hemisphere.

As for the sensors, the robot has two tilt sensors to measure its orientation and three gyroscopes to measure its angular velocity. Position of the robot with respect to the inertial frame is measured using a stereo vision system, Video Tracker G280 manufactured by OKK inc. The Video Tracker is capable of tracking bright or dark contrast markers, as well as calculating its x-y-z coordinates using a pair of CCD cameras. In this research, we attached three balls covered by reflection sheet to the body so that the Video Tracker can detect them under a sufficient light source. Then we can work out the 3D coordinates of the robot's center from the positions of the three balls.

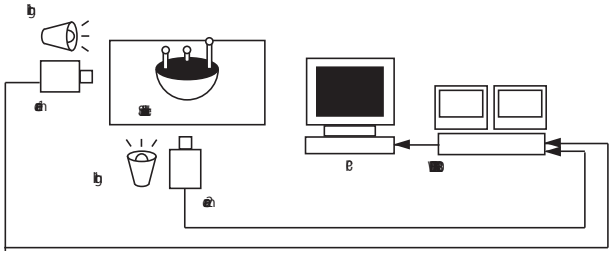

Fig. 12. Overview of the Experiment System

B. Parameter Identification

It is generally a difficult task to know the precise values of dynamic parameters, such as the mass, the mass distribution, the moment of inertia, friction coefficient and so on. Therefore, when we identify the Surface Walker, it is necessary to restrain the movement on 2D. We identify the parameters by fixing the constraining wheels on both sides of the Surface Walker.

Here, even if we constrain the movement of the Surface Walker, the model of the Surface Walker is nonlinear. It is more difficult to identify parameters of the nonlinear model than linear model. In this research, we obtain parameters of this nonlinear model by using a identification method called PSO. See [7] for detail.

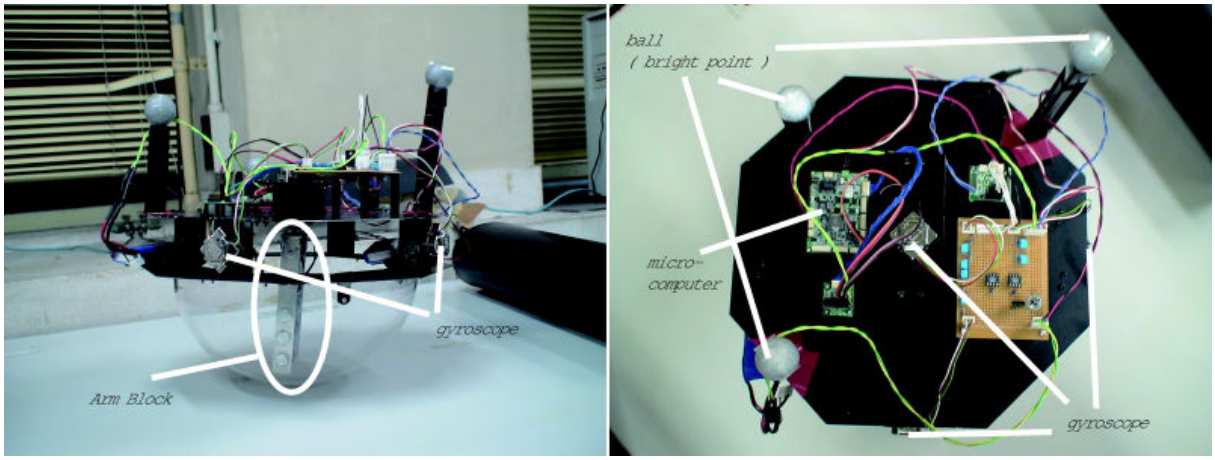

Fig. 11. The experimental setup

C. Experimental Result

Now we apply the same sort of oscillatory input as in the previous simulation to the real Surface Walker. Due to the physical limitations of the experimental system, we adopted the following input to the actuators.

$$\phi(t) = 0.890\sin(0.202t + \pi/2)[\mathrm{rad}] \quad (23)$$

$$\theta(t) = 0.157\sin(0.202t)[\mathrm{rad}] \quad (24)$$

The robot is expected to move straight in a certain direction, which depends on the transient behavior in the beginning.

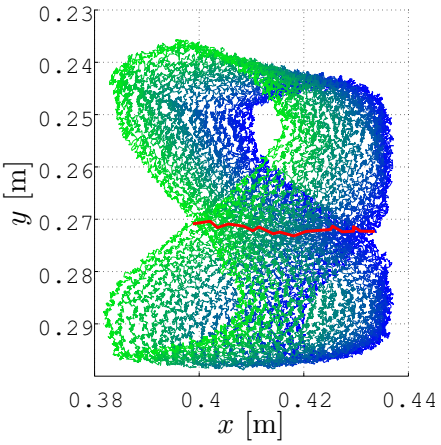

Fig. 13. Trajectory of the robot's position (x, y) in the experiment

Fig.13 shows the trajectory of the robot's position on the x-y plane in this experiment, which is a counterpart of Fig.8 in the simulation result. Though the locomotion is not quite fast, the robot slowly moves from right to left as the input cycle is repeated. The total travel was about $32[\mathrm{mm}]$ in 20 cycles.

V. Conclusion

In this research, we proposed a new kind of nonholonomic mobile robot utilizing rolling contact constraint, called the Surface Walker. We derived its dynamical model considering the rolling contact constraint and proposed a forwarding locomotion principle based on the nonholonomic motion planning with sinusoidal inputs, which was originally developed for kinematic models. Then we applied the proposed control inputs to the actual dynamical model. In spite of the discrepancy between the kinematic and dynamical models, we observed that the resulting motion eventually converges to a certain forwarding trajectory, both in numerical simulations and physical experiments.

Acknowledgements

The authors are grateful to anonymous reviewers for their valuable technical comments and corrections concerning the modeling section. This research was supported in part by the Grant-in-Aid for Young Scientists (B), No.19760285 of the Ministry of Education, Science, Sports and Culture, Japan, 2007–2009.

References

[1] S. Bhattacharya and S. K. Agrawal: Spherical Rolling Robot: A Design and Motion Planning Studies; IEEE Transactions on Robotics and Automation, Vol.116, No.6, pp.835-839(2000)

[2] J. Alves and J. Dias: Design and control of a spherical mobile robot; Proceedings of the Institution of Mechanical Engineers. Part I, Journal of Systems and Control Engineering, Vol.217, No.6, pp.457-467(2003)

[3] A. H. Javadi A. and P. Mojabi: Introducing Glory: A Novel Strategy for an Omnidirectional Spherical Rolling Robot; Journal of Dynamic Systems, Measurement, and Control, Vol.126, No.3, pp.678-683(2004)

[4] R. Mukherjee, M. A. Minor and J. T. Pukrushpan: Motion Planning for a Spherical Mobile Robot: Revisiting the Classical Ball-Plate Problem; Journal of Dynamic Systems, Measurement, and Control, Vol.124, No.4, pp.502-511(2002)

[5] H. Date, M. Sampei, M. Ishikawa, and M. Koga: Simultaneous Control of Position andOrientation for Ball-Plate Manipulation Problem Based on Time-State Control Form; IEEE Transactions on Robotics and Automation, Vol.20, No.3, pp.465-479(2004)

[6] Murray,R.M and Sastry,S.S.: Nonholonomic Motion Planning: Steering Using Sinusoids, IEEE Trans. on Automatic Control,Vol.38,No.5,pp.700-716 (1993).

[7] T. Wada, M. Ishikawa, R. Kitayoshi, I. Maruta and T. Sugie: Practical Modeling and System Identification of R/C Servo Motors , 2009 IEEE International Conference on Control Applications (CCA09; as a part of MSC2009), pp. 1378-1383(2009)